Nuclear Engineering and Technology 54 (2022) 2792–2800

Contents lists available at ScienceDirect

Nuclear Engineering and Technology

journal homepage: www.elsevier.com/locate/net

Original Article

Study on the effect of long-term high temperature irradiation on TRISO fuel

Asset Shaimerdenov [a, c, *], Shamil Gizatulin [a], Daulet Dyussambayev [a], Saulet Askerbekov [a, c], Shohei Ueta [b], Jun Aihara [b], Taiju Shibata [b], Nariaki Sakaba [b]

[a] The Institute of Nuclear Physics, 1 Ibragimov str., Almaty, 050032, the Republic of Kazakhstan
[b] Japan Atomic Energy Agency, 4002 Narita-cho, Oarai-machi, Higashiibaraki-gun, Ibaraki, 311-1393, Japan
[c] al-Farabi Kazakh National University, 71 al-Farabi av., Almaty, 050040, the Republic of Kazakhstan

ARTICLE INFO

Article history:
Received 20 October 2021
Received in revised form
26 January 2022
Accepted 27 February 2022
Available online 3 March 2022

Keywords:
TRISO
WWR-K
Graphite matrix
High burnup
Fuel integrity

ABSTRACT

In the core of the WWR-K reactor, a long-term irradiation of tristructural isotopic (TRISO)-coated fuel particles (CFPs) with a UO_2 kernel was carried out under high-temperature gas-cooled reactor (HTGR)-like operating conditions. The temperature of this TRISO fuel during irradiation varied in the range of 950–1100 °C. A fission per initial metal atom (FIMA) of uranium burnup of 9.9% was reached. The release of gaseous fission products was measured in-pile. The release-to-birth ratio (R/B) for the fission product isotopes was calculated. Aspects of fuel safety while achieving deep fuel burnup are important and relevant, including maintaining the integrity of the fuel coatings. The main mechanisms of fuel failure are kernel migration, silicon carbide corrosion by palladium, and gas pressure increase inside the CFP. The formation of gaseous fission products and carbon monoxide leads to an increase in the internal pressure in the CFP, which is a dominant failure mechanism of the coatings under this level of burnup. Irradiated fuel compacts were subjected to electric dissociation to isolate the CFPs from the fuel compacts. In addition, nondestructive methods, such as X-ray radiography and gamma spectrometry, were used. The predicted R/B ratio was evaluated using the fission gas release model developed in the high-temperature test reactor (HTTR) project. In the model, both the through-coatings of failed CFPs and as-fabricated uranium contamination were assumed to be sources of the fission gas. The obtained R/B ratio for gaseous fission products allows the finalization and validation of the model for the release of fission products from the CFPs and fuel compacts. The success of the integrity of TRISO fuel irradiated at approximately 9.9% FIMA was demonstrated. A low fuel failure fraction and R/B ratios indicated good performance and reliability of the studied TRISO fuel.

1. Introduction

The tristructural isotopic (TRISO)-coated fuel particle (CFP) is a nuclear fuel used in modern and newly designed high-temperature gas-cooled reactors (HTGRs). The initial concept for this type of CFP was introduced in the 1950s [1]. This TRISO fuel comprises a sphere with a diameter of not more than 1 mm. A typical TRISO fuel contains a fissile material in the center of the particle, called a kernel (mainly UO_2 or UCO, low-enriched uranium is used) with a diameter in the range of 350–600 μm. The kernel is covered with four coating layers: a low-dense pyrocarbon (PyC), high-dense PyC, silicon carbide (SiC), and high-dense PyC. The first low-dense PyC coating layer is a buffer that provides a void volume for the gaseous fission products and carbon–oxygen reaction products released from the fuel kernel. In addition, this layer accommodates swelling of the fuel kernel. The second coating layer of TRISO fuel is a dense, highly isotropic PyC layer. This layer protects the kernel from chloride-containing off-gas during SiC deposition and ensures that the gaseous fission products are retained in the particle. The third coating layer of SiC provides the main structural strength of the particle and acts as the main barrier to the release of nongaseous fission products that are not sufficiently retained by the pyrolytic carbon layer or within the kernel itself. The final coating layer of dense PyC protects the SiC layer during operation, acts as a surface for

* Corresponding author. The Institute of Nuclear Physics, 1 Ibragimov str., Almaty, 050032, Kazakhstan.
E-mail address: aashaimerdenov@gmail.com (A. Shaimerdenov).

https://doi.org/10.1016/j.net.2022.02.026

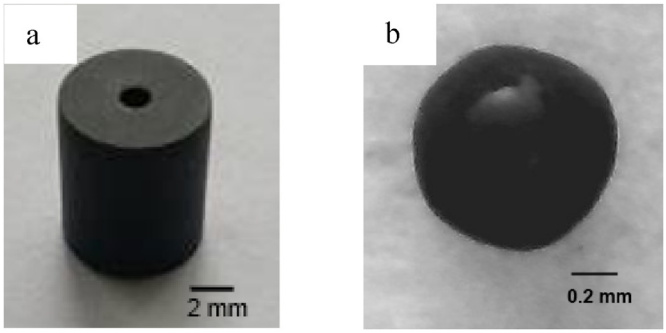

Fig. 1. (a) Fuel compact; (b) coated fuel particle.

bonding with the graphite matrix of the fuel, and provides an additional barrier to the release of gaseous fission products [2–7].

At present, HTGR technologies are being actively developed by China [8–10], Japan [11,12], Korea [13–15], Russia [16,17], and the United States [17–19]. The international community has expressed great interest in HTGRs because this type of reactor can make it possible to move to a clean energy future using hydrogen energy [20,21].

A common global task for all operating and designed reactors is ensuring their safety during both normal operation and emergency conditions. HTGRs are no exception, and thus research aimed at the development and qualification of materials and fuels with increased performance and safety are relevant and in demand. For example, in the roadmap for fourth-generation power systems (Gen-IV), one of the main tasks for the development of HTGR is to carry out research and development of materials and fuels that will can realize a burnup of 150–200 GWd/t-U at a temperature of 1000 °C [22].

The degradation and destruction of TRISO-coatings occur mainly because of the pressure of gaseous fission products, radiation-induced changes in the size of pyrolytic carbon, and chemical reactions leading to the corrosion of SiC [2,3]. Therefore, research on the fuel design, structural materials, and manufacturing technology based on ongoing experimental data continues to improve the operational characteristics. After a pilot batch of samples is manufactured, the samples are characterized, which includes testing the fuel under operating conditions. For HTGR, these conditions include a neutron field, helium environment, and high temperatures.

In this study, we investigated the effect of long-term high-temperature neutron irradiation on the integrity of TRISO fuel. Irradiation was carried out to achieve a maximum burnup of uranium of up to 10% fissions per initial metal atom (FIMA) as a target. During irradiation, the ratio of the gas release to the birth rate (R/B) was monitored to determine the degree of destruction of the fuel coatings during irradiation. In the post-irradiation examination, the fraction of failed fuel particles was determined.

The difference between this work and other similar works lies in the object of study and the conditions of the reactor experiment, i.e. different sizes of the particle kernel, the thickness of the protective layers, the fuel compact, the accumulated neutron fluence, the irradiation temperature and the achieved burnup. For example, in the AGR-2 experiments at the ATR reactor, a burnup of 9.01–10.69% FIMA was achieved and the accumulated neutron fluence was $3.05–3.53 \times 10^{25}$ n/m^2 at an irradiation temperature of 1335 K. The diameter of the fuel compact was 12.2 mm, and the height was 25 mm [23]. During the PYCASSO experiments at the HFR reactor, particles with a kernel diameter of 980 μm, a buffer layer thickness of 174 μm, and a SiC layer thickness of 63 μm were studied. The samples were irradiated at a temperature of 1273 K and the accumulated neutron fluence was $1.63–2.02 \times 10^{25}$ n/m^2 [24]. While operating the HTTR reactor, fuel compacts with a diameter of 26 mm and a height of 39 mm are used, with a particle kernel diameter of 600 μm, a buffer layer thickness of 60 μm, and a SiC layer thickness of 25 μm. During operation of the reactor, the average temperature is 1223 K. The maximum achieved burnup is 3.3% FIMA [25].

2. Experimental setup

2.1. Studied specimens

Three fuel compact specimens with TRISO-CFPs designed newly for burnup extension were fabricated and examined in the in-reactor and out-of-pile tests. The manufacturer of the fuel compacts and CFPs was Nuclear Fuel Industries, Ltd (see Fig. 1). The diameter of the fuel kernel was 500 μm (on HTTR – 600 μm), the thicknesses of the buffer and the SiC layers were 95 μm and 35 μm (on HTTR – 60 and 25 μm), respectively. The CFPs had a diameter of 0.92 mm (see Fig. 1 (b)). The fuel kernel was manufactured using the gel-precipitation method. Multiple coating layers were deposited in a fluidized bed via chemical vapor deposition. The CFPs were dispersed into a graphite matrix of a fuel compact. The fuel compact specimens comprised cylinders made by pressing the CFPs with graphite powder and a carbonized binder. The fuel production process is described in Ref. [25]. One fuel compact specimen contained approximately 550–660 CFPs. The technical specifications of the fuel compacts and CFPs are given in Tables 1 and 2, respectively. The fuel compact has a through hole in the center to compensation volume of gaseous uranium fission products.

The fraction of as-fabricated SiC-defective CFP in a fuel compact was between 0 and 1.8×10^{-3}, corresponding to the presence of 0–1 as-fabricated SiC-defective particles in each fuel compact. So, maximal possible SiC-defective CFPs are three particles for fuel compacts (estimated to contain a combined total of 1650–1980 CFPs) irradiated in this test. It is suggested that failure of the as-fabricated fuel may have occurred during the compacting process, as both the as-fabricated exposed uranium fraction and SiC-defective fraction of the loose CFP before the compacting process were at the level of as-fabricated uranium contamination, 9×10^{-7} [26]. The initial failure occurred because a special die (10mmOD x 2mmID x 12mmH) was applied which is smaller than one for the conventional HTTR fuel compact (26mmOD x 10mmID x 39mmH),

Table 1
Fuel compact specifications.

Item		Specification
Shape		Cylindrical
Spatial dimensions	Outer diameter [mm]	10.0 ± 0.2
	Inner diameter [mm]	2.0 + 0.3/-0.15
	Length [mm]	12.0 ± 0.2
Particle packing fraction [vol%]		25 + 5/-3
Chemical composition of fuel compact matrix	Carbon (Graphite powder & carbonized binder)	
Density of the fuel compact matrix [g/cm^3] (without coated fuel particles)	1.70 ± 0.05	

Table 2
Fuel particle specifications.

Item	Specification
Fuel kernel	
^{235}U enrichment (%)	9.9 ± 0.1
Diameter (μm)	500 ± 40
Density (g/cm^3)	10.63 ± 0.26
Chemical composition	UO_2
Coated Fuel Particle	
Layer thickness [μm]	
- Buffer	95 ± 30
- I-PyC	40 ± 8
- SiC	35 ± 5
- O-PyC	40 ± 6
Layer density (chemical composition) [g/cm^3]	
- Buffer (Pyrolytic carbon)	1.05 + 0.15/-0.05
- I-PyC (Pyrolytic carbon)	1.85 ± 0.10
- SiC (Silicon carbide)	≥3.19
- O-PyC (Pyrolytic carbon)	1.85 ± 0.10
- OPTAF (Pyrolytic carbon)[a]	≤1.03

[a] Optical Anisotropy Factor.

despite the lower packing fraction (24.9–26.0 vol%) than that of high-temperature test reactors (HTTRs) (30 vol%) [12].

2.2. Irradiation facility

The TRISO fuel specimens were irradiated in the WWR-K research reactor core. The WWR-K is a light water tank-type thermal reactor with a nominal power rating of 6 MW. Demineralized water serves as the moderator and coolant. Demineralized water and beryllium serve as the side reflectors. The enrichment of uranium-235 in the reactor fuel is 19.7% [27,28]. The reactor was commissioned in 1967 and converted to the use of low-enriched fuel in 2016. The reactor is intended for a variety of studies in the fields of fission and fusion materials science. In recent years, part of the experimental work at the reactor has been carried out in scientific cooperation with a number of research institutes in the Republic of Kazakhstan, the Russian Federation, and Japan, focusing on determining the properties of advanced materials under reactor irradiation conditions [29–35]. The maximum flux of thermal and fast neutrons in the irradiation position of the specimens were 1×10^{14} and 5×10^{13} cm^{-2}s^{-1}, respectively.

2.3. Irradiation capsule

The average water temperature in the core of the WWR-K reactor is 323 K; however, the operating conditions of the TRISO fuel in the HTGR are characterized by a high temperature (>1173 K) and a gaseous environment (helium coolant). To create such conditions in the WWR-K reactor, an experimental device (ED) was developed that could reproduce the conditions of the HTGR. The ED consists of an outer ampoule and an inner capsule. The outer ampoule is made of SAV-1 aluminum alloy. The inner capsule is made of a niobium–zirconium alloy. The ED is gas-swept, and the possibility for gas sampling during irradiation is available. The capsule is filled with helium (99.9999% purity). Gas sampling was performed periodically. The sampled gas was analyzed using a wide-range semiconductor gamma spectrometer. The volume of the sampled gas was 0.2 L.

The fuel compacts were stacked vertically and irradiated simultaneously [26]. The peak temperature of the fuel compact specimens during the test was 1323 ± 373 K. The temperature was recorded using six K-type thermocouples. To increase the temperature in the region of the specimens, molybdenum shields were placed between the outer ampoule and the inner capsule. The temperature was controlled by changing the helium pressure in the gap between the outer ampoule and inner capsule. The capsule design is shown in Fig. 2 (units: mm).

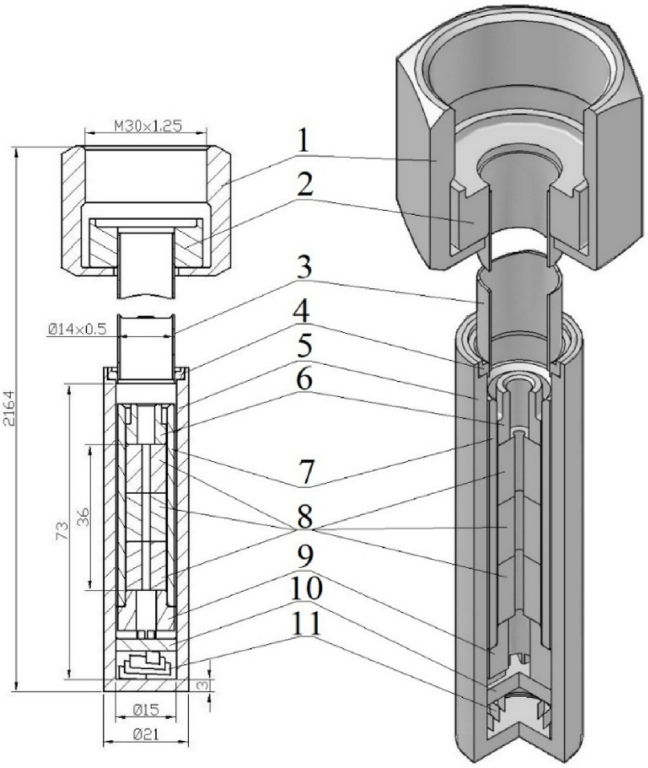

Fig. 2. Capsule (1 – the coupling nut; 2 – the nipple; 3 – pipe; 4 – adapting; 5 – barrel; 6, 7 – graphite bush; 8 – fuel compact; 9 – graphite bushing; 10 – graphite washer; 11 – telescope spring).

Predictions of the temperature levels during irradiation for the ED design under study were performed using ANSYS Fluent v.13 [36]. The estimated distribution of the temperature inside the ED at the beginning of the cycle (BOC) is shown in Fig. 3 (units: K). The maximum temperature at the center of the fuel compacts was approximately 1473 K. The capsule wall temperature was 913 K.

3. Results and discussion

3.1. In-situ study

Over the course of the irradiation of the TRISO fuel specimens, the gaseous fission products were sampled from the capsule. Then, the sampled gas was analyzed using a wide-range gamma spectrometer to determine the quantitative radionuclide composition of the sampled gas. The ED gas sampling system is illustrated in Fig. 4. The R/B was determined as an important parameter of the performance of the TRISO fuel. Gas sampling was carried out periodically and after the reactor achieved a steady-state condition; the system was filled with pure helium to the initial pressure after each sampling event.

The R/B value was measured using ^{88}Kr because it is free of the influence of the precursor nuclide. The predicted R/B value was evaluated using the fission gas release model developed in the HTTR project [37,38]. In the model, both failed CFP and as-fabricated uranium contamination were considered as sources of fission gas. The model considers two modes of fission gas release, namely diffusion and recoil, for each source. In addition, two forms of diffusion release are considered: in-grain and at the grain

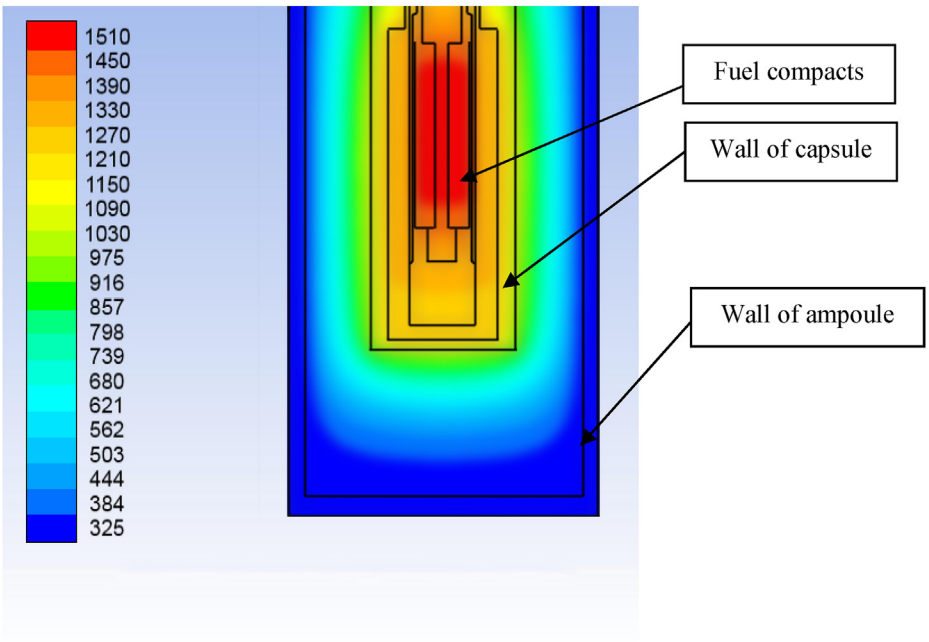

Fig. 3. Temperature distributions along the experimental device.

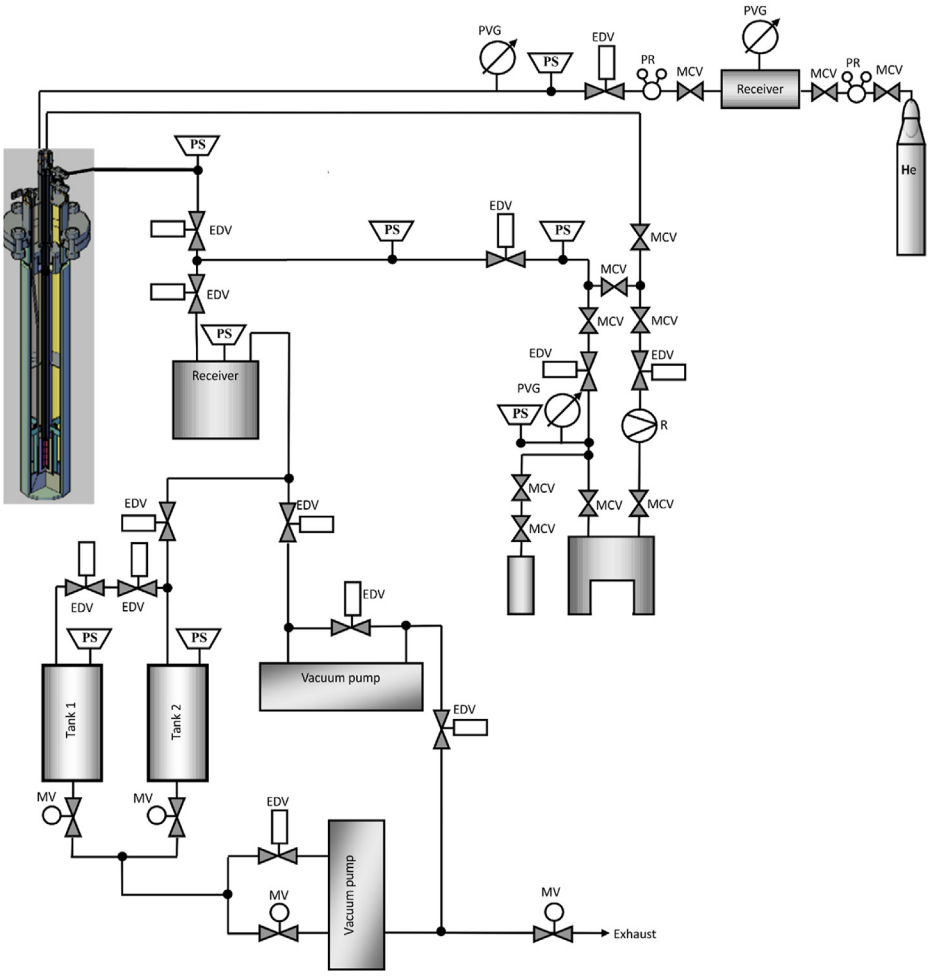

Fig. 4. Gas sampling system during irradiation test (EDV - electrically-driven valve; MCV - manually-controlled valve; PS - pressure sensor; MV - motor valve; PR – pressure regulator; PVG – pressure-vacuum gage; R - rotameter).

boundary. The parameters and equations used in this model are reported in detail in the literature. Finally, the R/B of ^{88}Kr is expressed as follows:

$$\frac{R}{B}=\left\{\left(f_{k,r}\times f_{m,d}\right)+\left(f_{k,d}\times f_{m,ad}\right)\right\}\times\phi_k+\left(f_{m,r}\times f_{m,d}\right)\times\phi_c, \tag{1}$$

where R/B is the fractional release of fission gases from the fuel compact, $f_{k,r}$ is the recoil release fraction from the kernel, $f_{m,d}$ is the fractional release from the fuel compact matrix, $f_{k,d}$ is the fractional release from the kernel by diffusion, $f_{m,ad}$ is the fractional release from the kernel by grain boundary diffusion, ϕ_k is the fraction of through-coating failed particles, $f_{m,r}$ is the recoil release fraction from the fuel compact matrix, and ϕ_c is the uranium contamination fraction in the fuel compact matrix.

The recoil release fraction from the kernel is calculated using the following equation [37]:

$$f_{k,r}=\frac{3}{4}\frac{R}{a}-\frac{1}{16}\left(\frac{R}{a}\right)^3, \tag{2}$$

where R is the recoil distance, and a is the kernel diameter.

The fractional release from the fuel compact matrix is calculated using the following equation, which takes into account the in-graphite grain diffusion and the graphite grain boundary diffusion releases [37]:

$$f_{m,d}=3\sqrt{\frac{D'}{\lambda}}\coth\left(\sqrt{\frac{\lambda}{D'}}-\sqrt{\frac{D'}{\lambda}}\right), \tag{3}$$

where D' is the reduced diffusion coefficient of nuclide in the fuel kernel, and λ is the decay constant.

The fractional release from the kernel by diffusion is calculated using the following equation [37]:

$$f_{k,d}=3\left(\frac{1}{\Gamma_1}\left(\frac{\coth\sqrt{\mu_1}}{\sqrt{\mu_1}}\right)+\frac{1}{\Gamma_2}\left(\frac{\coth\sqrt{\mu_2}}{\sqrt{\mu_2}}-\frac{1}{\mu_2}\right)\right)f_{BU}, \tag{4}$$

$$\Gamma_1=1-\frac{\mu_1}{\mu_2}, \tag{5}$$

$$\Gamma_2=1-\frac{\mu_2}{\mu_1}, \tag{6}$$

$$\mu_i=\frac{\lambda_i}{D_i'}, \tag{7}$$

where f_{BU} is the burnup correction factor.

The fractional release from the fuel compact through fission recoil from uranium contamination in the fuel compact matrix is calculated using the following equation [37]:

$$f_{m,r}=\frac{R(3(r_i+r_0)-2R)}{6\left(r_0^2-r_i^2\right)}, \tag{8}$$

where r_0 is the outer radius of the fuel compact, and r_i is the inner radius of the fuel compact.

The prediction was compared with the measurement data to determine the additional failure fraction of the CFP during irradiation. The measured R/B value of ^{88}Kr was calculated as follows:

$$A(t)=A_{sat}\{1-\exp(-\lambda t)\}, \tag{9}$$

$$A_{sat}=\frac{A(t_{smp})}{1-\exp(-\lambda t_{smp})}\ (t=t_{smp}), \tag{10}$$

$$\frac{dA(t)}{dt}=\lambda A_{sat}\{\exp(-\lambda t)\}, \tag{11}$$

$$R=\frac{dA(0)}{dt}=\lambda A_{sat}=\frac{\lambda A(t_{smp})}{1-\exp(-\lambda t_{smp})}, \tag{12}$$

$$B=\lambda\cdot\frac{W}{3.2\times10^{-11}}\cdot\frac{Y}{100}, \tag{13}$$

where $A(t)$ is the radioactivity (Bq) of ^{88}Kr at time t (s), λ is the decay constant of ^{88}Kr (6.88×10^{-5} s^{-1}), A_{sat} is the saturated radioactivity (Bq) of ^{88}Kr, t_{smp} is the sampling time (s) corresponding to a state of stable heat release from the fuel, R is the release rate (Bq/s) of ^{88}Kr, B is the birth rate (Bq/s) of ^{88}Kr, W is the heat (W) released from the fuel, and Y is the fission yield of ^{88}Kr (3.58%). For this analysis, the swept helium gas was sampled at a steady-state reactor power level after reaching ^{88}Kr saturation (which takes over five times longer than the half-life of ^{88}Kr, i.e., over 15 h after reaching a stable power level).

The measured R/B value of ^{88}Kr was compared with the predicted one, which was evaluated with as-fabricated uranium contamination (a fraction of 9×10^{-7}) and no additional fuel failure. Then, no initial failure was confirmed at the beginning of the irradiation. The measured R/B increased gradually without any additional fuel failure at 41–46 GWd/t-U. At approximately 69 and 78 GWd/t-U of burnup, the measured R/B value seemed to increase stepwise with levels corresponding to 1–2 through-coating CFP failures in accordance with the prediction. At this time, a leakage of helium out of the inner capsule was found, which enhanced heat removal from the fuel specimen. Therefore, because the evaluated power in the fuel specimen might be underestimated as a result of the above phenomena, it was suggested that the calculated R/B could be slightly overestimated. The calculated R/B values of ^{88}Kr for the entire irradiation time of the specimens are shown in Fig. 5 [26].

The difference between the experimental R/B data and the predicted data is most likely due to methodological aspects that

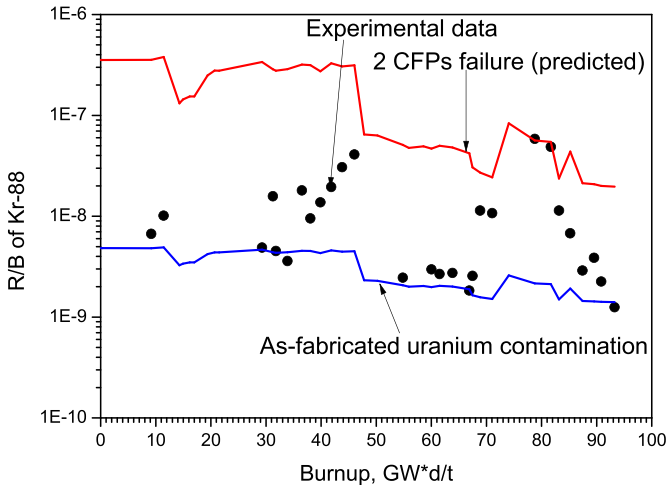

Fig. 5. R/B of ^{88}Kr variation during irradiation test [26].

Table 3
The scope of post-irradiation examinations.

PIE method	Instrumentation	Information obtained
Appearance observation	Lens	Visual inspection
Dimensional change	Mechanical micrometer MATRIX with the measurement uncertainty 0.01 mm	Swelling or shrinkage effect
Gamma spectrometry	Canberra GX-2518 germanium semiconductor gamma spectrometer	Determination of fuel failure fraction, fuel burnup
X-ray radiography	RPD-250 X-ray unit	Determination of fuel failure fraction

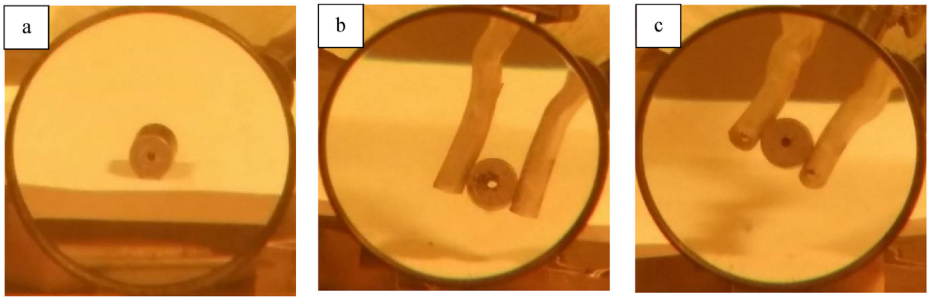

Fig. 6. (a) Fuel compact #65; (b) fuel compact #53; (c) fuel compact #69.

cannot be taken into account in a simulation. For example, after each gas sampling, the irradiation capsule was washed with pure helium. The presence of krypton-88 in the sampled gas even at low fuel burnup indicates that the particles have surface as-fabricated uranium contamination, which is also confirmed by the results of calculations.

3.2. Post-irradiation examination

The duration of irradiation of the specimens was 400 equivalent full power days (EFPDs). During this irradiation time, the average burnup in three compacts was 9.9% FIMA and the time-average temperature of 1264 K. The maximum accumulated fast neutron fluence ($E_n > 0.18$ MeV) was 0.83×10^{25} n/m^2.

After completion of the irradiation test, the ED was unloaded from the core and cooled in a pool. Then, it was dismantled and cut in a hot cell. The specimens were retrieved and identified for further study.

The scope of the post-irradiation examinations (PIEs) is summarized in Table 3.

Visual inspection revealed that the appearance of the compacts remained unchanged after irradiation. This can be seen by comparing the appearance of the samples shown in Figs. 1 and 6.

The diameter and height of the irradiated fuel compacts were measured using a mechanical micrometer. These dimensions were measured at several points. A detailed scheme of the measured points is given in Ref. [39]. The dimensional analysis showed that all the fuel compacts experienced shrinkage. The shrinkage of the fuel compacts due to neutron irradiation is presented in Table 4. The presented results are the average values for each measured parameter.

In the next stage, it was necessary to study the CFPs separately; therefore, they had to be separated from the graphite matrix of the fuel compact. Previous post-reactor studies of the TRISO fuel of the HTTR reactor [37] have shown that electrical dissociation is an effective method for separating CFPs from a graphite matrix. Therefore, based on the device used in the study of HTTR fuel, a device for the electrical dissociation and acid leaching (denoted as "DEDAL") was developed to examine the irradiated fuel compacts in this study [39].

The DEDAL is a thermostable glass beaker with a volume of 250 ml. The vessel is closed on the top by a cover made of Teflon and provided by a silicon thermal isolating layer. A platinum cathode, platinum–rhodium–platinum thermocouple, and condenser are installed on the cover. To eliminate short circuiting between the anode and cathode, a screen made of a fiberglass mesh structure is installed. The condenser collects the acid vapors during acid leaching. A fuel compact is installed on the anode through the orifice in the cover. The anode is covered by insulating material, except for a 10 mm section to allow insertion of the fuel compact. The cathode was installed in the central hole of the fuel compact. During the experiments, the DEDAL was installed on an electric plate inside a hot cell.

The dissociation and leaching proceeded as follows: the fuel compact was remotely installed in a heat-resistant beaker of DEDAL, which was filled with a 36% solution of nitric acid; then, the electric plate was turned on, the solution was heated, and an electric current was applied to the electrodes for 2.5–3 h. Then, the supply of current to the electrodes was stopped and the leaching of uranium from the failed CFPs was carried out for 24 h.

The density of the nitric acid solution (1.22 g/cm^3) was measured at room temperature before the start of the experiments. During electrical dissociation, the solution temperature was 353 K, while during leaching it was 368 K. The dissociation and leaching procedures were identical for all the fuel compacts. As a result of the experiments, the CFPs were separated from the graphite matrix

Table 4
Dimensions of compacts before and after irradiation.

Compact #	# 65		# 53		# 69	
	Before irradiation	After irradiation	Before irradiation	After irradiation	Before irradiation	After irradiation
Diameter, mm	10.1	9.95	10.1	9.92	10.1	9.93
Height, mm	12.0	11.86	12.0	11.86	12.0	11.87

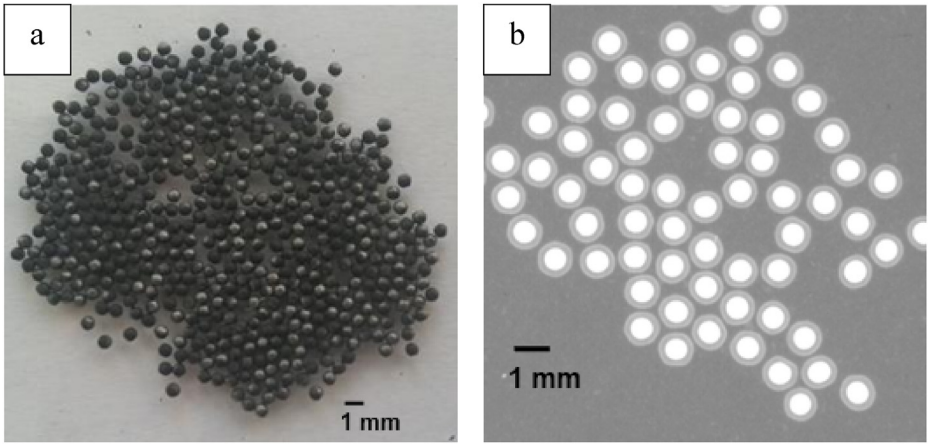

Fig. 7. (a) Photography of irradiated coated fuel particles after electric dissociation and acid leaching; (b) X-ray image of coated fuel particles after electric dissociation and acid leaching.

(Fig. 7 (a)), and uranium was leached from the CFPs with failed layers.

Gamma spectrometric analysis was performed to determine the fuel failure fraction. γ-ray measurements were obtained using a Canberra GX 2518 high-resolution germanium semiconductor coaxial wide-range (from 3 keV to 3 MeV) detector. The GX-2518 multi-channel semiconductor spectrometer measures the energies and relevant activities of the γ quanta emitted by radionuclides. The algorithms implemented in the spectrometer software make it possible to determine the radionuclide activity or specific activity in measured samples or objects, provided relevant measurement and calibration techniques are available.

The fuel failure fraction (F) is determined as follows:

$$F = \frac{A_i}{P_i X}, \tag{14}$$

where A_i is the total amount of fission product i in the leaching solution (Bq), P_i is the amount of fission product i in the CFP (Bq), and X is the number of CFPs in the fuel compact.

Individual CFPs and a solution of nitric acid containing a powdered mixture of the graphite matrix, fission products of uranium, and uranium leached from CFPs with failed layers were obtained after electrical dissociation. The nitric acid solution was filtered through a small mesh sieve. As a result, a solution of nitric acid and a mixture of graphite powder, uranium, and uranium fission products were obtained. A_i was determined as the sum of the activities of the fission products in the nitric acid solution and filtered powder. Only part of the solution and powder were analyzed using a gamma spectrometer. Note that the correction for radioactive decay was considered when determining the activity of A_i. Further, 10 CFPs with intact layers and a kernel were selected from each compact and analyzed using a gamma spectrometer. The selection of CFPs with intact layers and kernels was performed using X-ray radiography. In Equation (14), the average values of the activities of nuclides for the 10 CFPs were used for each fuel compact (P_i).

The main γ-ray nuclides of ^{106}Rh, ^{134}Cs, ^{137}Cs, ^{144}Ce, ^{144}Pr, ^{154}Eu and ^{155}Eu were detected in the CFPs. The fuel failure fraction was estimated based on the activity of ^{137}Cs. Cesium-137 was selected as the monitor because it has a long half-life, a small neutron capture cross-section, independence of the uranium fission yield on neutron energy, and absence in unirradiated fuel. The activities of other nuclides were determined with a greater error compared to the activity of ^{137}Cs, therefore they were not used to determine the fuel failure fraction. Unfortunately, it was not possible to estimate the fuel failure fraction based on the activity of uranium in the leached solution due to the high gamma background created by the uranium fission products. The measured (by 10 particles) and expected calculated values of the activity of cesium-137 in a particle and measured activity of cesium-137 in the leaching solution are shown in Table 5.

As a result, each of the irradiated fuel compacts seemed to contain more than 5–10% failed CFPs. The authors believe that this is possibly due to the fact that cesium-137, which was chosen as the burnup monitor, migrates from the fuel coating layers. In this study, the irradiated CFPs were cleaned directly by pressurized jet water after the electric deconsolidation to remove the adherent graphite matrix material from the CFPs. After this procedure, the CFPs were subjected to the leaching test. Therefore, there is a possibility that a few intact CFPs that survived the irradiation test were unintentionally broken and lost in the series of PIE procedures. The process of cleaning particles by pressurized jet water was necessary to remove fragments of the graphite matrix, which could later affect the measurement of the activity of particles and the calculation of their number. The large difference in the number of failure particles with the R/B data is due to the effect of destructive experiments on the structural integrity of the particles, therefore these data are overestimated.

The second method for determining the fuel failure fraction was x-ray radiography (see Fig. 7 (b)). X-ray radiography was performed using a portable RPD-250S unit. The high levels of radioactivity in the irradiated CFPs made it impossible to obtain high-quality X-ray images. Gamma emission from the CFPs darkened the roentgen

Table 5
Activity of ^{137}Cs in particle.

Compact ID	Measured average activity of ^{137}Cs in particle, Bq	Calculated activity of ^{137}Cs in particle, Bq	Measured average activity of ^{137}Cs in the leaching solution, Bq
65 (top)	4.5 10^6	3.8 10^6	$9.1 \cdot 10^7$
53 (mid)	4.0 10^6	1.5 10^6	$5.2 \cdot 10^7$
69 (bottom)	4.1 10^6	1.5 10^6	$6.4 \cdot 10^7$

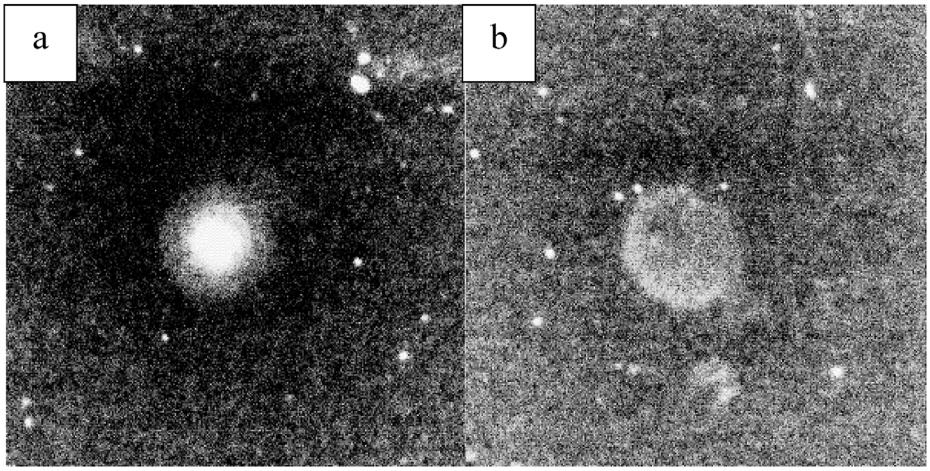

Fig. 8. (a) X-ray image of not failed CFPs; (b) X-ray image of failed CFPs.

Table 6
Result on number of CFP counted by X-ray radiography after the leaching test.

Compact ID	Number of intact CFPs observed after the leaching test	Number of sphere (CFP, kernel, coating without kernel) measured after irradiation	Number of the lost CFPs estimated by the leaching test	Number of the leached CFPs estimated by gamma spectroscopy of Cs-137 in nitric acid solution derived from Eq. 14
65 (top)	453	~497	~44	24
53 (mid)	503	~562	~59	35
69 (bottom)	512	~544	~32	29

film. To improve the X-ray images of the irradiated CFPs, a series of experiments with different X-ray modes were carried out. The current and voltage of the X-ray device, type of X-ray film, lead screens, and packaging design of the CFPs were varied. As a result, the optimal conditions for X-ray radiography were selected, which made it possible to determine the CFPs containing uranium unambiguously (see Fig. 8). Fig. 8 (a) clearly shows a bright glow in the center of the pebble. This confirms the presence of uranium in the particle. The integrity of the CFPs in each fuel compact was determined using X-ray images.

The number of CFPs counted by X-ray radiography after the leaching test is presented in Table 6.

In this study, it was concluded that the fuel failure fraction could not be determined by X-ray radiography or gamma spectrometric analysis. Therefore, we relied solely on the R/B data to qualify the fuel performance in this study.

Moreover, the differences in the sensitivity of fuel failure using the two methods (X-ray radiography and gamma spectrometric analysis) are most likely owing to the fact that some of the CFPs were completely damaged during dissociation and acid leaching. The number of failed CFPs determined by X-ray radiography was less than that determined by gamma spectrometric analysis.

Based on the R/B data, it can be argued that the new fuel design has good resistance to damage to the layers of the TRISO fuel until it reaches 10% FIMA burnup at an operating temperature of about 1264 K. situations). However, it is not known how it will behave when the temperature rises (for example, in emergency situations). Therefore, it is required to conduct a study of this fuel in transient conditions with elevated temperatures.

4. Conclusions

Irradiation of three fuel compacts with a graphite matrix was carried out in the WWR-K reactor. The fuel compacts consisted of newly designed TRISO-CFPs with a UO_2 kernel. CFP kernel and layers have different sizes compared to regular fuel used on HTTR. The maximum uranium burnup achieved in the TRISO fuel was 9.9% FIMA.

During irradiation of the fuel compacts, gas sampling was performed for radionuclide analysis. The experimental data obtained for the R/B ratio showed that the fuel retained its performance characteristics. The computational model based on the R/B ratio for predicting the number of failed fuel fractions indicated that at most two CFPs seemed to fail during irradiation. However, the obtained R/B data could be slightly overestimated. Note that the model developed for HTTR was used as the basis for the calculation model.

A suite of post-irradiation examinations of the fuel compacts with TRISO-CFPs was carried out. The integrity of the CFP layers was investigated using two methods: X-ray and gamma-spectrometric analyses. The fuel failure fraction could not be accurately determined because a few intact CFPs that survived the irradiation test would be unintentionally broken and lost during the PIE. Therefore, we relied solely on the R/B data to qualify the fuel performance in this study. On the other hand, the differences in the sensitivity of the fuel failure with the two different methods are most likely because some of the CFPs failed completely during dissociation and acid leaching.

The results of this study will be used in the future to develop a test procedure for a prototype of TRISO fuel specimens with a SiC matrix.

Funding

This work has been supported by Science Committee of the Ministry of Education and Science of the Republic of Kazakhstan, under the project AP08052726.

This work has been supported by International Science and Technology Center, Nur-Sultan, Kazakhstan, under the regular projects No. K-1797 and K-2222.

CRediT authorship contribution statement

Asset Shaimerdenov: Writing – original draft, Conceptualization, Investigation. **Shamil Gizatulin:** Data curation, Investigation, Supervision. **Daulet Dyussambayev:** Visualization, Investigation. **Saulet Askerbekov:** Formal analysis. **Shohei Ueta:** Resources, Methodology, Supervision. **Jun Aihara:** Methodology. **Taiju Shibata:** Supervision. **Nariaki Sakaba:** Supervision.

Declaration of competing interest

The authors declare that they have no known competing financial interests or personal relationships that could have appeared to influence the work reported in this paper.

References

[1] M.S. T Price, The Dragon Project origins, achievements and legacies, Nucl. Eng. Des. 251 (2012) 60–68.

[2] P.A. Demkowicz, et al., Coated particle fuel: historical perspectives and current progress, J. Nucl. Mater. 515 (2019) 434–450.

[3] M.J. Kania, H. Nabielek, H. Nickel, Coated particle fuels for high-temperature reactors, in: Materials Science and Technology, Wiley, 2015.

[4] D.A. Petti, et al., TRISO-coated particle fuel performance, in: R.J.M. Konings (Ed.), Comprehensive Nuclear Materials, 3, Elsevier, Amsterdam, 2012, pp. 151–213.

[5] High Temperature Gas Cooled Reactor Fuels and Materials, IAEA, TECDOC, 2010, p. 1645.

[6] K. Verfondern, H. Nabielek, J.M. Kendall, Coated particle fuel for high temperature gas cooled reactors, Nucl. Eng. Technol. 39 (2007) 603–616.

[7] D.A. Petti, et al., Key differences in the fabrication, irradiation and high temperature accident testing of US and German TRISO-coated particle fuel, and their implications on fuel performance, Nucl. Eng. Des. 222 (2003) 281–297.

[8] Zuoyi Zhang, Haitao Wang, Yujie Dong, Li Fu future development of Modular HTGR in China after HTR-PM, in: Proceedings of the HTR 2014 Weihai, China, October 27-31, 2014. Paper HTR2014-11456.

[9] Zuoyi Zhang, Yujie Dong, Li Fu, Zhengming Zhang, Haitao Wang, Xiaojin Huang, Li Hong, Bing Liu, Xinxin Wu, Hong Wang, Xingzhong Diao, Haiquan Zhang, Jinhua Wang, The Shandong Shidao Bay 200 MWe high-temperature gas-cooled reactor Pebble-bed Module (HTR-PM) demonstration power plant: an engineering and technological innovation, Engineering 2 (2016) 112–118.

[10] Xu Yuanhui, Hu Shouying, Li Fu, Yu Suyuan, High Temperature Reactor Development in China, Progress in Nuclear Energy, 47, 2005, pp. 260–270, https://doi.org/10.1016/j.pnucene.2005.05.026. Issues 1–4.

[11] K. Kunitomi, S. Katanishi, S. Takada, T. Takizuka, X. Yan, Japan's future HTR—the GTHTR300, Nucl. Eng. Des. 233 (1–3) (2004) 309–327, https://doi.org/10.1016/j.nucengdes.2004.08.026.

[12] Tetsuo Nishihara, X. Yan, Yukio Tachibana, Taiju Shibata, Hirofumi Ohashi, Shinji Kubo, Yoshitomo Inaba, Shigeaki Nakagawa, Minoru Goto, Shohei Ueta, Noriaki Hirota, Yoshiyuki Inagaki, Kazuhiko Iigaki, Shimpei Hamamoto, Kunitomi, Kazuhiko Excellent Feature of Japanese HTGR Technologies, JAEA-Technology, 2018, p. 182, https://doi.org/10.11484/jaea-technology-2018-004, 004.

[13] Young-WooLee, Park Ji-Yeon, Yeon, Kyung Ku Kim, Chae Jeong Woong, Ki Kim Bong, Goo Kim Young, Min Kim, Moon Sung Cho, Development of HTGR-coated particle fuel technology in Korea, Nucl. Eng. Des. 238 (2008) 2842–2853, https://doi.org/10.1016/j.nucengdes.2007.11.023.

[14] Won Jae Lee, Progress of nuclear hydrogen Program in Korea, in: Proceedings of the 3rd Nuclear Hydrogen Workshop Nuclear Hydrogen for Green Horizon, 2009, p. 29.

[15] Bong Goo Kim, Sunghwan Yeo, Kyung-Chai Jeong, Yeon-Ku Kim, Young Woo Lee, Moon Sung Cho, The first irradiation testing and PIE or TRISO-coated particle fuel in Korea, Nucl. Eng. Des. 329 (2018) 34–45, https://doi.org/10.1016/j.nucengdes.2018.01.037.

[16] V.I. Kostin, N.G. Kodochigov, S.E. Belov, A.V. Vasyaev, V.F. Golovko, A. Shenoj, Development of GT-MGR plant power conversion unit design, Atom. Energy 102 (1) (2007) 57–63.

[17] N.N. Ponomarev-Stepnoi, N.G. Abrosimov, A.V. Vasyaev, M.E. Ganin, V.F. Golovko, D.L. Zverev, V.V. Petrunin, Similarity of high-temperature gas-cooled reactor technologies and designs in Russia and USA, Atom. Energy 108 (2) (2010) 89–96, https://doi.org/10.1007/s10512-010-9261-8.

[18] C. Andrew, Kadak the status of the US high-temperature gas reactors, Engineering 2 (2016) 119–123.

[19] Paul A. Demkowicz, John D. Hunn, Scott A. Ploger, Robert N. Morris, Charles A. Baldwin, Jason M. Harp, Philip L. Winston, Tyler J. Gerczak, J. Isabella, van Rooyen, C. Fred, Montgomery, M. Chinthaka, Silva Irradiation performance of AGR-1 high temperature reactor fuel, Nucl. Eng. Des. 306 (2016) 2–13, https://doi.org/10.1016/j.nucengdes.2015.09.011.

[20] Marc A. Rosen, Seama Koohi-Fayegh the prospects for hydrogen as an energy carrier: an overview of hydrogen energy and hydrogen energy systems, Energ. Ecol. Environ. 1 (1) (2016) 10–29, https://doi.org/10.1007/s40974-016-0005-z.

[21] Karl Verfondern Nuclear Energy for Hydrogen Production 58, 2007, p. 199.

[22] Technology Roadmap Update for Generation IV Nuclear Energy Systems, OECD Nuclear Energy Agency, Europe, 2014.

[23] P. Blaise, Collin AGR-2 Irradiation Test Final As-Run Report, 2014. INL/EXT-14-32277.

[24] Liu Dong, Steven Knol, Jon Ell, Harold Barnard, Mark Daviese, A. Jan, Vreeling, O. Robert, Ritchie, X-ray tomography study on the crushing strength and irradiation behaviour of dedicated tristructural isotropic nuclear fuel particles at 1000 °C, Mater. Des. 187 (2020) 108382, https://doi.org/10.1016/j.matdes.2019.108382.

[25] S. Ueta, J. Aihara, N. Sakaba, M. Honda, N. Furihata, K. Sawa, Fuel performance under continuous high-temperature operation of the HTTR, J. Nucl. Sci. Technol. 51 (2014) 1345–1354, 11-12: R&D for HTGR technology utilizing Japan's HTTR.

[26] Shohei Ueta, Jun Aihara, Asset Shaimerdenov, Daulet Dyussambayev, Shamil Gizatulin, Petr Chakrov, Nariaki Sakaba Irradiation test and post irradiation examination of the high burnup HTGR fuel, in: Proceeding of 8th International Topical Meeting on High Temperature Reactor Technology, HTR, USA, 2016, pp. 246–252. November 6-10, 2016 Las Vegas, NV.

[27] A.A. Shaimerdenov, F.M. Arinkin, Sh Kh Gizatulin, D.S. Dyussambayev, S.N. Koltochnik, P.V. Chakrov, L.V. Chekushina, Conversion of WWR-K research reactor to LEU fuel, Atom. Energy 123 (2017) 15–20, https://doi.org/10.1007/s10512-017-0294-0.

[28] A.A. Shaimerdenov, D.A. Nakipov, F.M. Arinkin, et al., Phys. Atom. Nuclei 81 (2018) 1408, https://doi.org/10.1134/S1063778818100162.

[29] I. Tazhibayeva, M. Skakov, V. Baklanov, E. Koyanbayev, A. Miniyazov, T. Kulsartov, E. Nesterov, Study of properties of tungsten irradiated in hydrogen atmosphere, Nucl. Fusion 57.12 (2017) 126062.

[30] Y. Chikhray, V. Shestakov, O. Maksimkin, L. Turubarova, I. Osipov, T. Kulsartov, K. Tsuchiya, Study of Li2TiO3+ 5 mol% TiO2 lithium ceramics after long-term neutron irradiation, J. Nucl. Mater. 386 (2009) 286–289.

[31] P. Blynskiy, Y. Chikhray, T. Kulsartov, M. Gabdullin, Z. Zaurbekova, G. Kizane, A. Shaimerdenov, Experiments on tritium generation and yield from lithium ceramics during neutron irradiation, Int. J. Hydrogen Energy 46 (13) (2021) 9186–9192.

[32] T. Kulsartov, Z. Zaurbekova, M. Gabdullin, E. Nesterov, N. Varlamova, A. Novodvorskiy, A. Evdakova, Simulation of hydrogen isotopes absorption by metals under uncompensated pressure conditions, Int. J. Hydrogen Energy 44.55 (2019) 29304–29309.

[33] I.L. Tazhibayeva, T.V. Kulsartov, Y.Y. Baklanova, Z.A. Zaurbekova, Y. Gordienko, V. Y, Ponkratov Reactor studies of tritium release from lead-lithium eutectic Li15. 7Pb with deuterium over the sample, Nuclear Mater. Energy 25 (2020) 100868.

[34] I.L. Tazhibayeva, T.V. Kulsartov, Z. Zaurbekova, Y. Gordienko, V. Y, Ponkratov Reactor studies of hydrogen isotopes interaction with lithium CPS using dynamic sorption technique, Fusion Eng. Des. 146 (2019) 402–405.

[35] L. Chekushina, D. Dyussambaev, A. Shaimerdenov, K. Tsuchiya, T. Takeuchi, H. Kawamura, T. Kulsartov, Properties of tritium/helium release from hot isostatic pressed beryllium of various trademarks, J. Nucl. Mater. 452 (1–3) (2014) 41–45.

[36] ANSYS FLUENT UDF Manual, ANSYS Inc. – Release 14.0. – USA, 2011, p. 592.

[37] S. Ueta, J. Sumita, K. Emori, M. Takahashi, K. Sawa, Fuel and fission gas behavior during rise-to-power test of the high temperature engineering test reactor (HTTR), J. Nucl. Sci. Technol. 40 (2003) 679.

[38] S. Ueta, M. Umeda, K. Sawa, S. Sozawa, M. Shimizu, Y. Ishigaki, H. Obata, Preliminary test results for post irradiation examination on the HTTR fuel, J. Nucl. Sci. Technol. 44 (2007) 1081.

[39] Asset Shaimerdenov, Shamil Gizatulin, Yergazy Kenzhin, Daulet Dyussambayev, Shohei Ueta, Jun Aihara, Taiju Shibata investigation of irradiated properties of extended burnup TRISO fuel, in: Proceeding of 9th International Topical Meeting on High Temperature Reactor Technology (HTR 2018), Warsaw, Poland, Paper HTR, October 8-10, 2018, 2018-182.